FOIL DEPRESSION FACTORS FOR DISC-SHAPED

DETECTORS

APPROVED:

E. Leigh Secrest
Major Professor

H. C. Parrish
Minor Professor

L. F. Connell Jr.
Director of the Department of Physics

Jack Johnson
Dean of the Graduate School

FOIL DEPRESSION FACTORS FOR DISC-SHAPED DETECTORS

THESIS

Presented to the Graduate Council of the
North Texas State College in Partial
Fulfillment of the Requirements

For the Degree of

MASTER OF SCIENCE

by

Tom Lewis Gallagher, B. A.

Fort Worth, Texas

June, 1954

TABLE OF CONTENTS

LIST OF TABLES

LIST OF ILLUSTRATIONS

CHAPTER I

INTRODUCTION

The comparatively new field of neutron physics has introduced many problems arising from the detection and quantitative measurement of these minute nucleons. It has become necessary to investigate and evaluate by theoretical means some of the errors which arise from the inherent qualities of the materials used in experimental procedures. An important method of obtaining neutron measurements has been the use of foil materials which absorb neutrons and subsequently become radioactive. The rate of emission of product particles from the reaction may be measured, and from a knowledge of the absorptive qualities of the detector an estimate of the incident neutron flux can be obtained.

Because of the absorptive qualities of a detector, the neutron density to be measured will be lowered.[1] The ratio of the average neutron current density incident on the surface of the detector to the average current density in the same region in the absence of the detector is defined as the foil depression factor. By the use of the depression factor a compensation for this error may be made. If the detector is placed in a flux of fast neutrons, the neutron density is

---

[1] N. Bothe, Zeit. f. Phys. 120, 437 (1943).

only very slightly depressed, since the supply of neutrons is constantly replenished;[2] but if the detector is placed in a flux of thermal neutrons, the depression may be considerable.

A treatment of flux depression due to a spherical detector has been presented by Bothe[3] and revised by Tittle[4] to fit more nearly experimental results. Corinaldesi[5] investigated the depression for a plain infinite detector. These authors also presented associated solutions for disc-shaped detectors. Workman[6] calculated depression factors for disc-shaped detectors using oblate spheroidal coordinates. Trammell,[7] using solutions of the diffusion equation in oblate spheroidal coordinates which did not depend upon the density inside the detector, calculated a foil depression factor for a disc-shaped detector which agreed with the experimental data of Bothe.

Workman and Trammell, with whom the writer has had the pleasure to work personally, worked more in an exploratory manner, making many of the "blind alley" calculations and investigating many less profitable numerical methods, thereby making a more straightforward task of the determination of foil depression factors. The generalized data

---

[2] Ibid., 437.

[3] Ibid., 437.

[4] C. W. Tittle, Nucleonics 9, 60 (1951).

[5] E. Corinaldesi, Nuovo Cim. 3, 131 (1946).

[6] B. J. Workman, "A Method for Calculating Foil Depression Factors," Unpublished Master's Thesis, Department of Physics, North Texas State College (June, 1953).

[7] M. R. Trammell, "Neutron Density Depression Due to An Oblate Spheroidal Detector," Unpublished Master's Thesis, Department of Physics, North Texas State College (January, 1954).

which are presented in this thesis are the culmination of the determination of the foil depression factor using oblate spheroidal coordinates.

CHAPTER II

THEORY

1. The Density Function

The measurement of a neutron flux by means of a detector is made difficult by the fact that the very presence of the detector depresses the flux in its vicinity, thus leading to a low response by the detector. This depression is dependent upon the size, shape, and composition of the detector. The medium between the neutron source and the detector also has a considerable influence on the degree of depression. The absorption of neutrons both within the detector and intervening medium is dependent upon the energy of the neutrons as well as upon their direction.

1.1. The general solution.--Let us consider an infinite homogeneous medium which produces neutrons at a rate Q neutrons per second per cubic centimeter and which may absorb them. Let us further assume that these neutrons are in thermal equilibrium with the surrounding medium. It is then possible to assume an average energy for the neutrons. The neutron density in the medium is given by[1]

$$\left[-\frac{\lambda_t}{3}\nabla^2 + \Sigma_a\right] \Psi = Q, \qquad (1)$$

---

[1] S. Glasstone and M. C. Edlund, The Elements of Nuclear Reactor Theory (D. Van Nostrand Co., Inc., New York, 1952), first edition, p. 101.

where λ_t is the transport mean free path, and Σ_a is the macroscopic absorption cross section of the medium. If a detector were introduced into the field, the equation for the density in its interior would be analogous.

A disc-shaped detector can be satisfactorily approximated by oblate spheroidal coordinates.[2] In this system the shape of the detector is determined by μ which fixes the eccentricity of an ellipse, and by f the interfocal distance of the ellipse which determines the radius of the detector for a given μ. Rotation about the minor axis gives the desired effect of a disc. Figure 1 shows the relation between the oblate spheroidal and the rectangular coordinate systems.

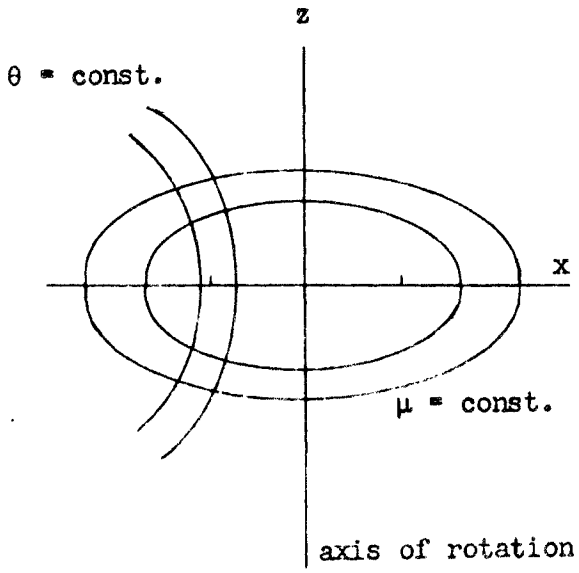

$x = \frac{1}{2} f \cosh\mu \sin\theta \cos\varphi$

$y = \frac{1}{2} f \cosh\mu \sin\theta \sin\varphi$

$z = \frac{1}{2} f \sinh\mu \cos\theta$

f = distance between foci

$= 2(a^2 - b^2)^{\frac{1}{2}}$

$2a$ = major axis

$2b$ = minor axis

Fig. 1.—Coordinate system

---

[2] P. M. Morse and H. Feshbach, Methods of Theoretical Physics, Part II (McGraw-Hill Book Co., New York, 1953), first edition, p. 1502.

In oblate spheroidal coordinates Eq. (1) becomes

$$\frac{1}{\cosh\mu}\frac{\delta}{\delta\mu}\cosh\mu\frac{\delta\varphi}{\delta\mu}+\frac{1}{\sin\theta}\frac{\delta}{\delta\theta}\sin\theta\frac{\delta\varphi}{\delta\theta}-c^2(\cos^2\theta+\sinh^2\mu)\varphi=0, \qquad (2)$$

where $\varphi = f - \frac{Q}{\Sigma a}$ and $c^2=\frac{1}{4}\left(\frac{j\Sigma_a}{\lambda_Q}\right)f^2$.

Assuming the product solution

$$\varphi = R(\mu)\,S(\theta)$$

and separating the equations, we get

$$\frac{1}{\cosh\mu}\frac{d}{d\mu}\cosh\mu\frac{dR}{d\mu}-(B+c^2\sinh^2\mu)R=0 \qquad (3)$$

$$\frac{1}{\sin\theta}\frac{d}{d\theta}\sin\theta\frac{dS}{d\theta}+(B-c^2\cos^2\theta)S=0, \qquad (4)$$

where B is the separation constant. Making the substitutions

$$\xi = i\sinh\mu \quad \text{and} \quad \eta = \cos\theta \qquad (5)$$

we get for the separated equations

$$\frac{d}{d\xi}(1-\xi^2)\frac{dR}{d\xi}+(B-c^2\xi^2)R=0 \qquad (6)$$

$$\frac{d}{d\eta}(1-\eta^2)\frac{dS}{d\eta}+(B-c^2\eta^2)S=0. \qquad (7)$$

These equations are seen to be identical. Their general solutions will, of course, be the same, but the ranges of the two variables are different, since $i0_+ \leq \xi \leq i\infty$ and $-1 \leq \eta \leq +1$. The solutions to be used will differ, since they must be analytic in different regions of the complex plane.

When $c^2 = 0$, Eq. (6), or Eq. (7), is simply Legendre's equation; hence we try to find solutions in the form

$$R = \sum_m r_m Q_m(\xi) \tag{8}$$

$$S = \sum_m s_m P_m(\eta), \tag{9}$$

where $P_m(\eta)$ and $Q_m(\xi)$ are Legendre polynomials. These particular choices are made since $P_m(\eta)$ is well-behaved for $-1 \leq \eta \leq +1$, whereas $Q_m(\xi)$ is not; and $Q_m(\xi)$ is well-behaved for all pure imaginary positive ξ, whereas $P_m(\eta)$ diverges at $\eta = i\infty$. If we substitute Eq. (8) into Eq. (6), we find that the coefficients r_m satisfy the equation

$$f(m)r_{m-2} + [g(m) - B]r_m + h(m)\, r_{m+2} = 0, \tag{10}$$

where

$$f(m) = \frac{m(m-1)c^2}{2(m-3)(2m-1)}$$

$$g(m) = \frac{(2m^2 + 2m - 1)c^2}{(2m-1)(2m+3)} + m(m+1)$$

$$h(m) = \frac{(m+1)(m+2)c^2}{(2m+5)(2m+3)}.$$

The coefficients $\underline{s}_m$ satisfy the same equation since the $\underline{P}_m$'s satisfy the same recurrence relations as the $\underline{Q}_m$'s.

For the case $c^2 = 0$, Eq. (10) reduces to

$$[B - m(m + 1)]\, r_m = 0,$$

which implies that unless $B = k(k + 1)$ where $k = 0, 1, 2, \ldots,$ all the $\underline{r}_m$'s vanish. If $B = k(k + 1)$, $r_m = 0$, if $m \neq k$, but $\underline{r}_k$ is arbitrary, as it must be since our differential equation is just Legendre's equation in this case. In general the $\underline{r}_m$'s will be solutions of the system

$$\begin{aligned}
[g(0) - B]\, r_0 + h(0) r_2 &= 0 \\
f(2) r_0 + [g(2) - B]\, r_2 + h(2) r_4 &= 0 \\
f(4)\, r_2 + [g(4) - B]\, r_4 + h(4) r_6 &= 0 \\
\cdot \quad \cdot \quad \cdot & \\
\cdot \quad \cdot \quad . &
\end{aligned} \tag{11}$$

In order that the system of Eq. (11) be compatible its secular determinant must vanish, that is,

$$\begin{vmatrix}
g(0) - B & h(0) & 0 & 0 \\
f(2) & g(2) - B & h(2) & 0 \\
0 & f(4) & g(4) - B & h(4) \\
0 & 0 & \circ & \circ
\end{vmatrix} = 0. \tag{12}$$

Let us denote the infinite set of roots of Eq. (12) by $B_0, B_1, B_2, \ldots, B_k, \ldots$. Let us call $\underline{d}_m^k$ the set of $\underline{r}_m$'s corresponding to $\underline{B}_k$. The system of Eqs. (11) determines the ratio of the $\underline{d}_m^k$'s only; one member of each set is still arbitrary. We see that for even $\underline{k}$ only even $\underline{m}$'s occur, and for $\underline{k}$ odd only odd $\underline{m}$'s occur. The secular determinant, for the case when $c^2 = 0$, reduces to the infinite product

$$\prod_{k=0}^{k=\infty} [k(k+1) - B] = 0, \tag{13}$$

and the roots $\underline{B}_k$ are simply $B_k = k(k+1)$ just as we had expected. In this case $d_m^k = 0$ unless $m = k$, and is arbitrary in this case. For reasonably small values of $\underline{c}^2$, we expect $\underline{d}_k^k$ to be the most important member of the set $\underline{d}_m^k$. Let us set

$$B_k = k(k+1) + b_k, \tag{14}$$

where $\underline{b}_k$ is a function of $\underline{c}^2$ and tends to zero with $\underline{c}^2$. Consider the matrix in Eqs. (11) constructed around the k^{th} row:

$$\begin{aligned} f(k-2)d_{k-4}^k + \left[g(k-2) - B_k\right] d_{k-2}^k + h(k-2)d_k^k &= 0 \\ f(k)d_{k-2}^k + \left[g(k) - B_k\right] d_k^k + h(k)d_{k+2}^k &= 0 \\ f(k+2)d_k^k + \left[g(k+2) - B_k\right] d_{k+2}^k + h(k+2)d_{k+4}^k &= 0. \end{aligned} \tag{15}$$

For reasonably small values of $\underline{c}^2$ we can solve Eqs. (15) by assuming the expansion of Eq. (14) and by retaining only $\underline{d}_m^k$ with m = k, k ± 2, k ± 4 in Eqs. (15).

For $\underline{c}^2$ tending to zero the functions $\underline{R}_k$ must behave in the same manner as $\underline{Q}_k$, and the functions $\underline{S}_k$ must behave as $\underline{P}_k$. For this reason we pick $\underline{d}_k^k$ in each case such that $R_k(0) = Q_k(0)$ for even $\underline{k}$, and $\frac{d}{d\xi} R_k(0) = \frac{d}{d\xi} Q_k(0)$ for odd $\underline{k}$. An analogous choice is made for the functions $\underline{S}_k$. This also insures that $\underline{S}_k$ and $\underline{P}_k$ will match at the boundary $\mu = 0$.

Finally, the solution exterior to an oblate spheroidal detector can be expressed in the form

$$\Psi = \Psi_0 + \sum_k A_k R_k(\xi) S(\eta) \tag{16}$$

where the $\underline{A}_k$'s must be chosen so as to satisfy the appropriate boundary conditions, and $\underline{\Psi}_0$ is the solution in the absence of the foil ($\Psi_0 = \frac{Q}{\sum a}$). It will prove more convenient to define $\underline{\Psi}$ in terms of the constants $C_k = \frac{2R_k(0)A_k}{\Psi_0}$, that is to say,

$$\Psi = \Psi_0 \left(1 + \tfrac{1}{2}\sum_k C_k \frac{R_k(\xi)}{R_k(0)} \; S_k(\eta)\right). \tag{17}$$

Due to the symmetry of the foil about its central plane, only the even functions of η can be allowed; hence we may rewrite Eq. (17) as

$$\Psi = \Psi_0 \left(1 + \tfrac{1}{2}\sum_k C_{2k} \frac{R_{2k}(\xi)}{R_{2k}(0)} \; S_{2k}(\eta)\right), \tag{18}$$

and the summation extends over all positive integral values of $\underline{k}$.

1.2. The boundary conditions.--In order to achieve unique solutions we must insure that both the neutron flux density and the neutron current density are continuous at the boundary of the medium and the detector. By the use of the construct of the "albedo," which is defined for a surface to be[3]

$$a = \frac{\Psi - \frac{2\lambda_t}{3}\frac{\delta\Psi}{\delta n}}{\Psi + \frac{2\lambda_t}{3}\frac{\delta\Psi}{\delta n}}, \tag{19}$$

where n is a coordinate in the normal direction to the surface, we may insure these continuity conditions. Physically, the albedo of a surface represents the probability that a neutron will be reflected upon striking the surface. In the case of a diffuse thermal field it can be shown that this definition is equivalent to the reflection coefficient calculated from current densities as in Eq. (19). The albedo of a foil can be determined experimentally.[4] For thin foils we may designate the effective thickness by $\mu = \mu_0 = 0$ or $\xi = \xi_0 = 0$, that is to say, negligible thickness with a finite absorption. Under this assumption, we get[5]

$$\frac{\delta\Psi}{\delta n} = \frac{2i}{f|\eta|}\left(\frac{\delta\Psi}{\delta\xi}\right)_{\xi = 0}. \tag{20}$$

---

[3]Glasstone and Edlund, op. cit., p. 130.

[4]Ibid., p. 129.

[5]Morse and Feshbach, op. cit., Part I, p. 662.

A substitution of Eq. (20) into Eq. (19) yields

$$(1 - a)\Psi(0,\eta) = \frac{2i\lambda_t}{3R} \frac{(1 + a)}{|\eta|} \frac{\delta\Psi(0,\eta)}{\delta\xi} . \tag{21}$$

With the definitions $\rho = \frac{R}{\lambda_t}$ and $\beta = \frac{2}{3\rho}\left(\frac{1 + a}{1 - a}\right)$, Eq. (21) reduces to

$$|\eta|\ \Psi(0,\eta) = i\beta \frac{\delta}{\delta\xi} \Psi(0,\eta). \tag{22}$$

In writing Eqs. (19), (20), and (21) we have neglected the "exprapolated end point" or "augmentation distance."[6] We shall see later in Chapter III that the magnitude of this correction will be determined for us in a rather striking fashion!

1.3. The final solution.--The results of Sections 1.1 and 1.2 may be combined to yield the density function for the medium surrounding the detector. Substitution of Eq. (18) into Eq. (22) yields,

$$|\eta| + \tfrac{1}{2}\Sigma_k C_{2k} |\eta| S_{2k}(\eta) = \frac{i\beta}{2}\Sigma_k C_{2k} \frac{\frac{dR_{2k}(0)}{d\xi}}{R_{2k}(0)} S_{2k}(0). \tag{23}$$

Multiplication of Eq. (23) by $S_{2k}(\eta)$ and a subsequent integration over η gives the set of equations

---

[6]Glasstone and Edlund, op. cit., p. 104.

$$\sum_k \left(\underline{K}_{mk} + \beta\gamma_{2k}\delta_{mk} \right) C_{2k} = -2L_{m0}, \quad m = 0, 1, 2, \cdots, \tag{24}$$

where

$$\underline{K}_{mk} = \sum_p \sum_q d_{2p}^{2m} d_{2q}^{2k} I_{pq} \qquad N_{2k} = 2\sum_p \frac{(d_{2p}^{2k})^2}{4p+1}$$

$$I_{pq} = \int_0^1 z\, P_{2p}\, P_{2q}\, dz \qquad L_{m0} = \sum_p d_{2p}^{2m} I_{p0}$$

$$\gamma_{2k} = -\frac{N_{2k}}{2} \frac{R'_{2k}(0)}{R_{2k}(0)} \qquad \delta_{mk} = \begin{cases} 0, & m \neq k \\ 1, & m = k \end{cases}.$$

Eqs. (24) form a set of infinite equations which for all practical purposes may be approximated by the first five terms C_0, C_2, C_4, C_6, and C_{10}. A high speed computer may be used for this matrix solution, or if such a computer is not readily available, one may use the method of iteration. This iteration is successfully performed if Eqs. (24) are written

$$C_0 = -\frac{\left(2L_{00} + \underline{K}_{01} C_2 + \underline{K}_{02} C_4 + \underline{K}_{03} C_6 + \underline{K}_{04} C_8 + \underline{K}_{05} C_{10} \right)}{\underline{K}_{00} + \beta\gamma_0}$$

$$C_2 = -\frac{\left(2L_{10} + \underline{K}_{10} C_0 + \underline{K}_{12} C_4 + \underline{K}_{13} C_6 + \underline{K}_{14} C_8 + \underline{K}_{15} C_{10} \right)}{\underline{K}_{11} + \beta\gamma_2} \tag{25}$$

$$C_4 = -\frac{\left(2L_{20} + K_{20}\,C_0 + K_{21}\,C_2 + K_{23}\,C_6 + K_{24}\,C_8 + \underline{\overline{K}}_{25}\,C_{10}\right)}{\underline{\overline{K}}_{22} + \beta\gamma_4}$$

$$C_6 = -\frac{\left(2L_{30} + K_{30}\,C_0 + K_{31}\,C_2 + K_{32}\,C_4 + K_{34}\,C_8 + K_{35}\,C_{10}\right)}{\underline{\overline{K}}_{33} + \beta\gamma_6}$$

$$C_8 = -\frac{\left(2L_{40} + K_{40}\,C_0 + K_{41}\,C_2 + K_{42}\,C_4 + K_{43}\,C_6 + K_{45}\,C_{10}\right)}{\underline{\overline{K}}_{44} + \beta\gamma_8}$$

$$C_{10} = -\frac{\left(2L_{50} + K_{50}\,C_0 + K_{51}\,C_2 + K_{52}\,C_4 + K_{53}\,C_6 + K_{54}\,C_8\right)}{K_{55} + \beta\gamma_{10}},$$

where we have solved the first equation for C_0, the second equation for C_2, the third equation for C_4, etc. To a first approximation we solve the first equation for C_0 neglecting the coefficients C_2, C_4, C_6, C_8, C_{10}. This value for C_0 is substituted into the second equation and C_2 is gotten, neglecting the terms containing C_4, C_6, C_8, and C_{10}. This process is repeated until a single value is gotten for all the coefficients C_{2k}. The values of C_2, C_4, C_6, C_8, and C_{10} are now substituted into the first equation, and another, more accurate, value for C_0 is obtained. Successive substitution and re-evaluation will give the coefficients to the accuracy of the original matrix elements when a repetition of the values of C_{2k} occurs.

2. The Foil Depression Factor

The number of neutrons absorbed by a foil is proportional to the number of neutrons falling on its surface; therefore the flux depression is also proportional to the number of incident neutrons. The foil depression factor is always less than unity and is defined as the ratio of the number of neutrons actually incident on the surface $\mu = 0$ to the number of neutrons incident on the surface if no detector is present. By the use of the definition of the current density the depression factor $\underline{F}$ becomes

$$F = \frac{\frac{1}{4}\int_{-1}^{+1} \frac{f}{2}|\eta|\,\Psi(0,\eta) + \frac{2}{3}\lambda_t \frac{\delta\Psi}{\delta\xi}(0,\eta)\ d\eta}{\frac{1}{4}\int_{-1}^{+1} \frac{f}{2}\,|\eta|\,\Psi_0\,d\eta}\ . \tag{26}$$

Using the results from Sections 1.1, 1.2, and 1.3, we get for the foil depression factor

$$F = 1 + \sum_n C_{2n}\left(\underline{K}_{n0} + \frac{2}{3\rho}\frac{R'_{2n}(0)}{R_{2n}(0)}\,d_0^{2n}\right)\ . \tag{27}$$

In Chapter III $\underline{F}$ is calculated for several values of the variables shown in Eq. (27).

CHAPTER III

NUMERICAL RESULTS

In the preceding chapter the general theory of the solution of the diffusion equation and the subsequent determination of a foil depression factor were presented. Numerical calculations have been made with water as a medium for variable foil albedos from 0.5 to 1.0. By a slight adjustment of parameters it is possible to convert these data to a medium of paraffin or of graphite. The numerical tabulation in Section 2 is rounded off to four significant figures for brevity. Most of the calculations were originally carried out to eight significant figures.

1. General Parameters

From the results of Chapter II, Section 2, it is apparent that $\underline{F}$ is dependent upon the $\underline{C}_{2k}$'s, $\rho = \frac{R}{\lambda_t}$, and the $\underline{d}_m^k$'s. The $\underline{d}_m^k$'s and the $\underline{C}_{2k}$'s are in turn dependent on $\underline{c}^2$. The $\underline{C}_{2k}$'s depend also upon the albedo $\underline{a}$ of the foil. From Section 1.1 we recall that $c^2 = 3 \Sigma_a \Sigma_s R^2$ where $\underline{\Sigma}_a$ and $\underline{\Sigma}_s$ refer to the medium. In order to tabulate numerical results from Chapter II in a useful form, it is necessary to compile this collection of variables into a set of dimensionless parameters.

After many "trial and error" sets were tried, the set $\underline{c}$, $\underline{\varepsilon}$, and $\underline{a}$ were found to be best suited for purposes of tabulation.

A choice of the medium surrounding the foil fixes $\underline{\varepsilon}$ which is defined as $\varepsilon^2 = 3\frac{\Sigma_a}{\Sigma_s}$. A selection of $\underline{c}$ and $\underline{\varepsilon}$ in turn fixes $\underline{R}$ since $\varepsilon\rho = c$. Finally a selection of the albedo $\underline{a}$ fixes the other variables of the problem. The numerical calculations have been made for water ($\varepsilon = 0.154$), for $0.5 \leq a \leq 1.0$ in steps of 0.1, and for $0.0 \leq c \leq 1.0$. A slight adjustment of the parameters made it possible to adapt these data for paraffin and graphite as well.

2. Method of Calculation

A "flow diagram" was made showing the order in which calculations were made and the component quantities of each factor. It was found that a diagram such as this is very helpful when cumbersome numerical data must be evaluated; duplication of factors is eliminated and a clear, although sometimes discouraging, understanding of the problem is obtained. The flow diagram is shown in Figure 2.

The separation constants $\underline{B_m}$ are tabulated in Table 1.

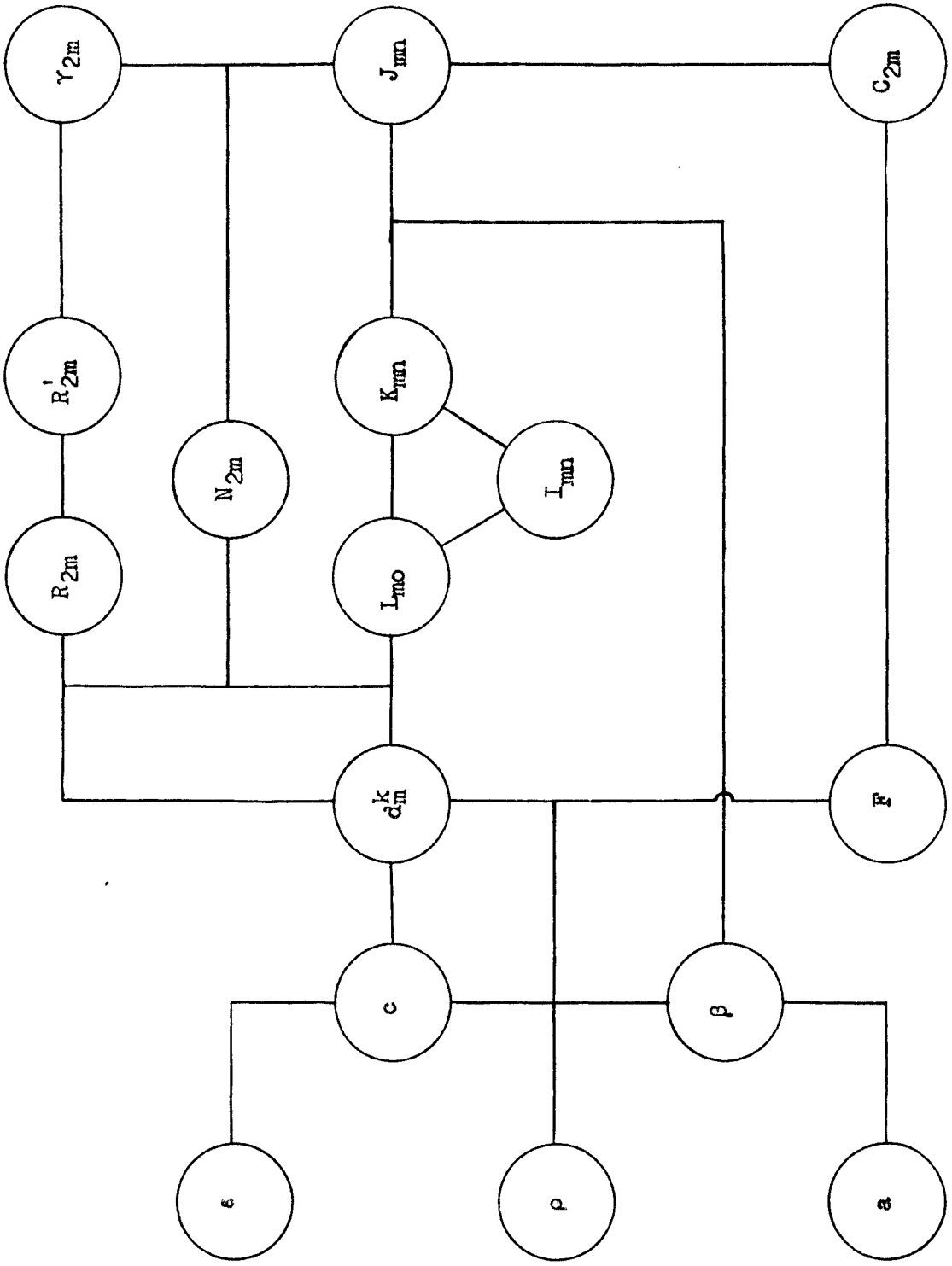

Fig. 2.--Flow diagram

TABLE 1

THE SEPARATION CONSTANTS B_m

m \ c	.1	.2	.4	.5	.6	.8	1.0
4	20.0051	20.0203	20.0811	20.1267	20.1814	20.3249	20.5160
6	42.0891	42.0201	42.0805	42.1258	42.1812	42.3223	42.5038
8	72.0048	72.0194	72.0775	72.1211	72.1744	72.3101	72.4846
10	110.0050	110.0200	110.0802	110.1253	110.1804	110.3208	110.5014

The values of $\underline{f}(m)$, $\underline{g}(m)$, $\underline{h}(m)$, $\underline{P_m}(0)$, $\underline{Q_m}(0)$, and $\underline{Q_m'}(0)$ are tabulated in Table 2.

TABLE 2

THE VALUES $f(m)$, $g(m)$, $h(m)$, $P_m(0)$, $Q_m(0)$, AND $Q_m'(0)$

m	$f(m)c^2$	$g(m)$	$h(m)c^2$	$P_m(0)$	$iQ_m(0)$	$iQ_m'(0)$
0	0	$.3333c^2$	.1333	1.0000	-1.5708	1.0000
2	.6667	$6+.5238c^2$	.1905	- .5000	.7854	-2.0000
4	.3429	$20+.5065c^2$	.2098	.3750	- .5890	2.6667
6	.3030	$42+.5030c^2$	.2196	- .3125	.4909	-3.2000
8	.2872	$72+.5018c^2$	.2256	.2734	- .4295	3.6571
10	.2786	$110+.5011c^2$	.2296	- .2461	.3866	-4.0635
12	.2733	$156+.5008c^2$	.2324	.2256	- .3543	4.4329

The coefficients $\underline{d}_m^k$ are tabulated in Table 3. It was necessary to use more than the diagonal term and the two immediately adjacent terms in some cases. (See page 21.)

The values of $\underline{R}_{2m}(0)$ and $\underline{R}'_{2m}(0)$ are tabulated below in Table 4.

TABLE 4

THE VALUES OF $R_{2m}(0)$ AND $R'_{2m}(0)$

c	.1	.2	.4	.5	.6	.8	1.0
$-iR_0$	1.5708	1.5708	1.5708	1.5708	1.5708	1.5708	1.5708
iR_2	.7853	.7854	.7854	.7854	.7854	.7854	.7854
$-iR_4$	.5890	.5890	.5890	.5890	.5890	.5890	.5890
iR_6	.4909	.4909	.4909	.4909	.4909	.4909	.4910
$-iR_8$	.4295	.4295	.4295	.4295	.4295	.4295	.4307
iR_{10}	.3866	.3866	.3866	.3866	.3866	.3866	.3866
iR'_0	1.0017	1.0066	1.0264	1.0410	1.0587	1.1026	1.1569
$-iR'_2$	2.0004	2.0037	2.0153	2.0239	2.0345	2.0612	2.0959
iR'_4	2.6670	2.6680	2.6722	2.6753	2.6791	2.6888	2.7011
$-iR'_6$	3.2002	3.2008	3.2031	3.2048	3.2070	3.2124	3.2200
iR'_8	3.6573	3.6577	3.6592	3.6603	3.6618	3.6654	3.6799
$-iR'_{10}$	4.0636	4.0639	4.0650	4.0658	4.0668	4.0693	4.0728

TABLE 3

THE COEFFICIENTS d_m^k

c /	.1	.2	.4	.5	.6	.8	1.0
d_0^0	.9994	.9978	.9912	.9864	.9805	.9661	.9484
$-d_2^0$	.001110	.004429	.01753	.02718	.03877	.06728	.1019
d_4^0	...	...	.00004802	.0001162	.0002385	.0007339	.001732
d_6^0	...	...	...	...	...	...	.0000124
d_0^2	.0002222	.0008887	.003552	.005547	.007981	.01416	.02204
d_2^2	1.0003	1.0010	1.0042	1.0065	1.0093	1.0163	1.0251
$-d_4^2$	.00000245	.0009806	.003936	.006164	.008903	.01595	.02516
d_6^2	...	...	...	.00001297	.00002698	.00008595	.0002119
d_0^4	...	...	...	...	.00001176	.00003713	.00009054
d_2^4	.0001361	.0005444	.002180	.003408	.004912	.008762	.01370

TABLE 3--Continued

c	.1	.2	.4	.5	.6	.8	1.0
d_4^4	1.00006662	1.0002665	1.0011	1.001670	1.0023	1.0042	1.0064
$-d_6^4$	.0001377	.0005511	.002206	.003449	.004970	.008855	.01387
d_8^4	...	...	...	...	.00000988	.00003129	.00007713
d_2^6	...	...	...	...	...	.00002071	.00005065
d_4^6	.00009499	.0003812	.001526	.002386	.003437	.006115	.009568
d_6^6	1.00002998	1.0001223	1.0004911	1.0007674	1.001106	1.001921	1.003160
$-d_8^6$	.00009599	.0003829	.001532	.002395	.003450	.006139	.009604
d_{10}^6	...	...	...	...	...	.00001610	.00003935
d_4^8	...	...	...	...	...	...	.00002969
d_6^8	.00007320	.0002928	.001172	.001831	.002638	.004692	.007357
d_8^8	1.00001766	1.00007069	1.0002829	1.0004424	1.0006375	1.001135	1.004427

TABLE 3--Continued

c	.1	.2	.4	.5	.6	.8	1.0
$-d_{10}^{8}$	.00007332	.0002933	.001173	.001834	.002641	.004697	.007362
d_{12}^{8}	...	...	...	...	...	...	.00002395
d_{8}^{10}	.00005935	.0002374	.0009499	.001484	.002138	.003802	.005943
d_{10}^{10}	1.00001149	1.00004600	1.0001839	1.0002874	1.0004139	1.0007361	1.001151
$-d_{12}^{10}$	.00005941	.0002376	.0009507	.001486	.002140	.003805	.005948

The factors γ_{2m} and N_{2m} are shown in Table 5.

TABLE 5

THE FACTORS γ_{2m} AND N_{2m}

c	.1	.2	.4	.5	.6	.8	1.0
γ_0	.6370	.6380	.6420	.6445	.6482	.6558	.6640
γ_2	.5095	.5113	.5175	.5222	.5279	.5427	.5624
γ_4	.5031	.5035	.5051	.5063	.5078	.5115	.5163
γ_6	.5015	.5017	.5024	.5030	.5037	.5054	.5078
γ_8	.5009	.5010	.5014	.5017	.5021	.5031	.5071
γ_{10}	.5006	.5007	.5009	.5011	.5014	.5020	.5029
N_0	1.9978	1.9911	1.9652	1.9461	1.9235	1.8684	1.8030
N_2	.4000	.4008	.4034	.4053	.4076	.4136	.4214
N_4	.2222	.2223	.2227	.2230	.2233	.2241	.2252
N_6	.1538	.1539	.1540	.1541	.1542	.1544	.1548
N_8	.1176	.1177	.1177	.1177	.1178	.1179	.1187
N_{10}	.0952	.0952	.0953	.0953	.0953	.0954	.0955

The factor β relates the albedo and the dimensionless radius. These values are listed in Table 6.

TABLE 6

THE COEFFICIENTS β

a \ c	.1	.2	.4	.5	.6	.8	1.0
.5	3.0800	1.5400	.7700	.6160	.5133	.3850	.3080
.6	4.1067	2.0533	1.0267	.8213	.6844	.5133	.4107
.7	5.8178	2.9089	1.4544	1.1635	.9696	.7272	.5818
.8	9.2400	4.6200	2.3100	1.8480	1.5400	1.1550	.9240
.9	19.5067	9.7533	4.8767	3.9013	3.2511	2.4383	1.9507

Table 7 is a tabulation of the integrals I_{mn}. It is obvious from symmetry that $I_{mn} = I_{nm}$.

The coefficients K_{mn} are also symmetric so that it is only necessary to tabulate a portion of them. They are tabulated in Table 8.

A coefficient related to K_{mn} is L_{mo} which is tabulated in Table 9.

The foil depression factors F for water medium are tabulated in Table 10.

The foil depression factors for media of paraffin and graphite may be obtained from Table 10 using the adjustments for c and a as shown in Table 11.

TABLE 7

THE INTEGRALS I_{mn}

m \ n	0	1	2	3	4	5	6
0	.50000	.125000	-.0208335	.0078125	-.0039063	.0022787	-.0014649
1	.12500	.125000	.033854	-.0062500	.0025391	-.0013486	.0008240
2	-.0208335	.033854	.070315	.0201825	-.00374355	.00153025	-.00082060
3	.0078125	-.0062500	.0201825	.048827	.014496	-.00270585	.00110780
4	-.0039063	.0025391	-.00374355	.014496	.037385	.011340	-.00213095
5	.0022787	-.0013486	.00153025	-.00270585	.011340	.0302815	.93230
6	-.0014649	.0008240	-.00082060	.00110780	-.00213095	.93230	.025423

TABLE 8

THE COEFFICIENTS K_{mn}

mn \ c	.1	.2	.4	.5	.6	.8	1.0
00	.4992	.4967	.4869	.4798	.4714	.4509	.4267
10	.1249	.1248	.1241	..1234	.1229	.1212	.1193
20	-.0208	-.0209	-.0210	-.0211	-.0212	-.0215	-.0218
30	.0078	.0078	.0078	.0078	.0079	.0079	.0079
40	-.0039	-.0039	-.0039	-.0039	-.0039	-.0039	-.0039
50	.0023	.0023	.0023	.0023	.0023	.0023	.00289
11	.1251	.1254	.1267	.1276	.1288	.1317	.1356
21	.0339	.0339	.0340	.0343	.0341	.0343	.0346
31	-.0062	-.0063	-.0063	-.0063	-.0063	-.0064	-.0065
41	.0025	.0025	.0025	.0025	.0025	.0026	.0026
51	-.0013	-.0013	-.0013	-.0013	-.0014	-.0014	-.0014
22	.0703	.0704	.0705	.0706	.0709	.0711	.0716
32	.0202	.0202	.0202	.0202	.0202	.0203	.0203
42	-.0037	-.0037	-.0037	-.0038	-.0038	-.0038	-.0038
52	.0015	.0015	.0015	.0015	.0015	.0015	.0015

TABLE 8--Continued

mn \ c	.1	.2	.4	.5	.6	.8	1.0
33	.0488	.0488	.0489	.0489	.0490	.0491	.0492
43	.0145	.0145	.0145	.0145	.0145	.0145	.0146
53	-.0027	-.0027	-.0027	-.0027	-.0027	-.0027	-.0027
44	.0374	.0374	.0374	.0374	.0374	.0375	.0378
54	.0113	.0113	.0113	.0113	.0113	.0114	.0114
55	.0303	.0303	.0303	.0303	.0303	.0303	.0304

TABLE 9

THE COEFFICIENTS λ_{mo}

m \ c	.1	.2	.4	.5	.6	.8	1.0
0	.4996	.4983	.4934	.4899	.4854	.4746	.4614
1	.1251	.1256	.1274	.1287	.1303	.1344	.1397
2	-.0208	-.0208	-.0206	-.0205	-.0203	-.0199	-.0193
3	.0078	.0078	.0078	.0078	.0078	.0077	.0077
4	-.0039	-.0039	-.0039	-.0039	-.0039	-.0039	-.0039
5	.0023	.0023	.0023	.0023	.0023	.0023	.0023

TABLE 10

THE FOIL DEPRESSION FACTORS FOR WATER MEDIUM

a \ c	.1	.2	.4	.5	.6	.8	1.0
.5	1.0464	.8635	.6552	.5924	.5467	.4895	.4622
.6	1.0367	.8871	.7026	.6433	.5988	.5408	.5113
.7	1.0271	.9127	.7580	.7048	.6633	.6068	.5757
.8	1.0179	.9399	.8238	.7804	.7452	.6945	.6642
.9	1.0088	.9689	.9029	.8759	.8527	.8169	.7934

TABLE 11

PARAMETER ADJUSTMENTS FOR F

	Water	Paraffin	Graphite
c	.1	.106	.035
	.2	.212	.070
	.4	.423	.140
	.5	.529	.174
	.6	.635	.209
	.8	.846	.279
	1.0	1.058	.349
a	.5	.520	.022
	.6	.617	.165
	.7	.714	.328
	.8	.810	.517
	.9	.905	.737

The graphs of foil depression factor F versus c for constant a for water, paraffin, and graphite are shown in Figures 3a, 4a, and 5a. Plots of F versus a for constant c are shown in Figures 3b, 4b, and 5b.

3. Discussion of Results

The augmentation distance that was referred to in Chapter II, Section 1.2, may be readily obtained from Figures 3a or 4a. It is obvious from these graphs that for all values of albedo there is effectively no depression for $c = 0.13$. This can be interpreted as implying an effective augmentation distance of $c = 0.13$, which in turn corresponds to $0.80\lambda_t$. This value is intermediate to the value of $2/3\ \lambda_t$ for a plane surface and the value of $4/3\ \lambda_t$ for a surface of infinite curvature.[1] In using the curves of Figures 3, 4, and 5, for experimental corrections one should compute c from the relation

$$c = 0.13 + \frac{R}{\lambda_t},$$

where R is the actual radius of the foil.

The data of Bothe have been plotted in Figure 6 and the corresponding theoretical data are shown. By choosing c to correspond to the disc radius of 0.7 cm. and 1.4 cm. values of F were found for different a using Figure 4a. It can readily be seen that the experimental and theoretical results check to within the accuracy of the experiment.

---

[1] Glasstone and Edlund, op. cit., p. 104.

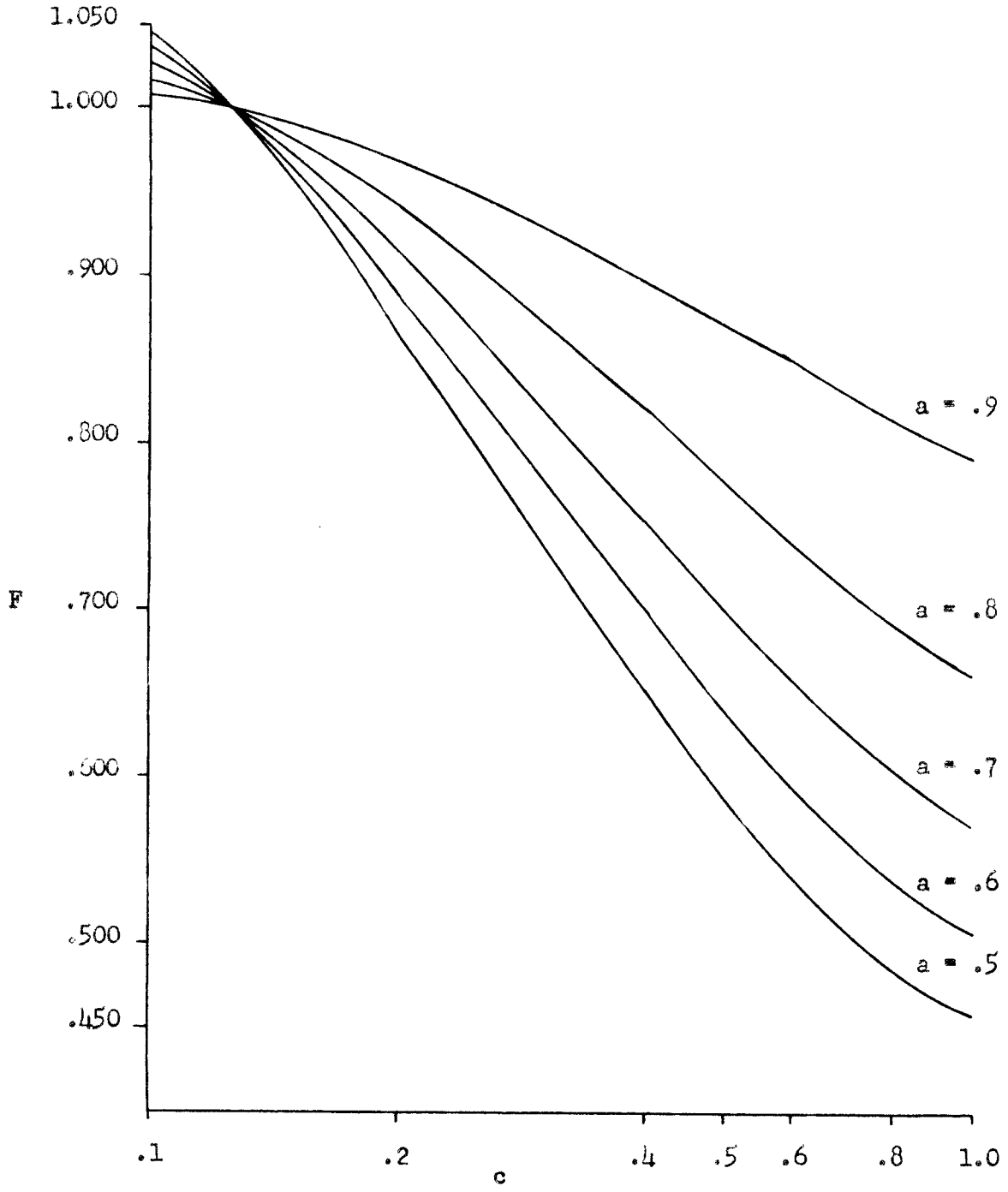

Fig. 3a.--F vs. c with constant a (water medium)

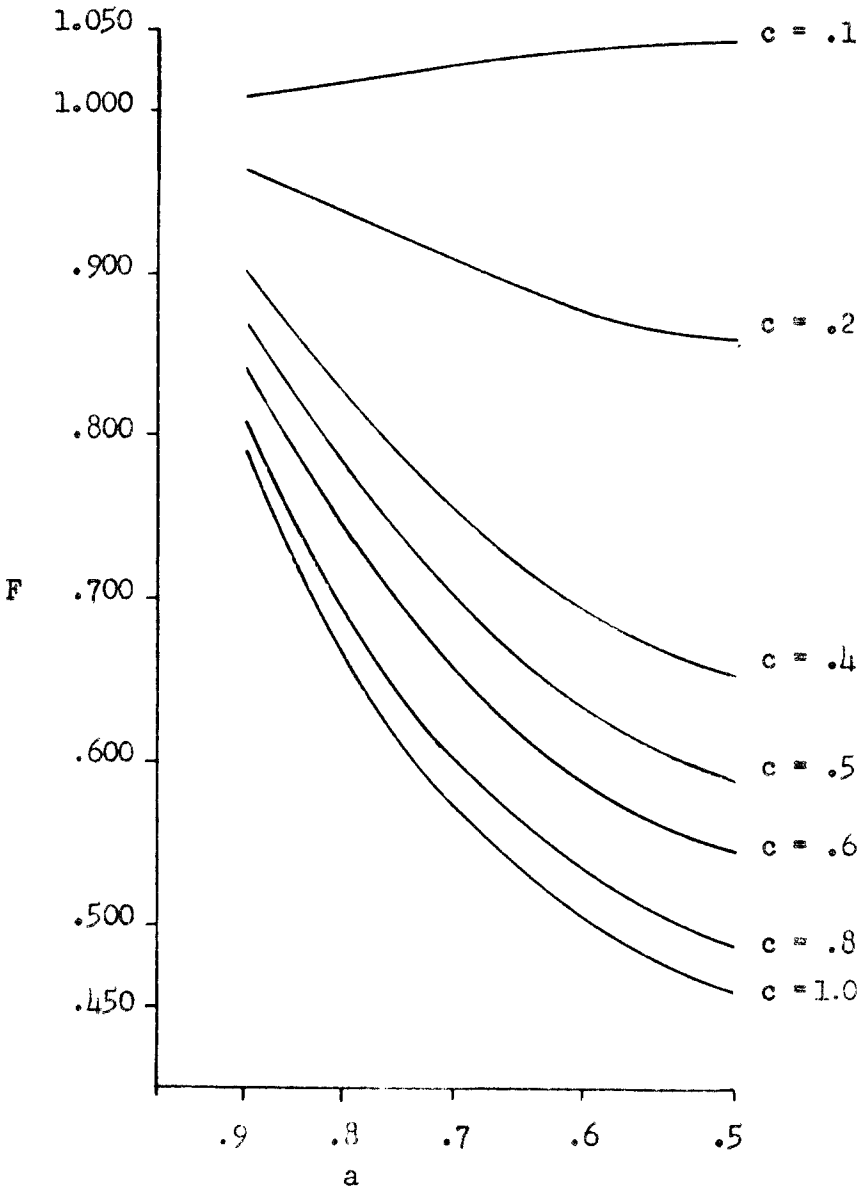

Fig. 3b.--F vs. a with constant c (water medium).

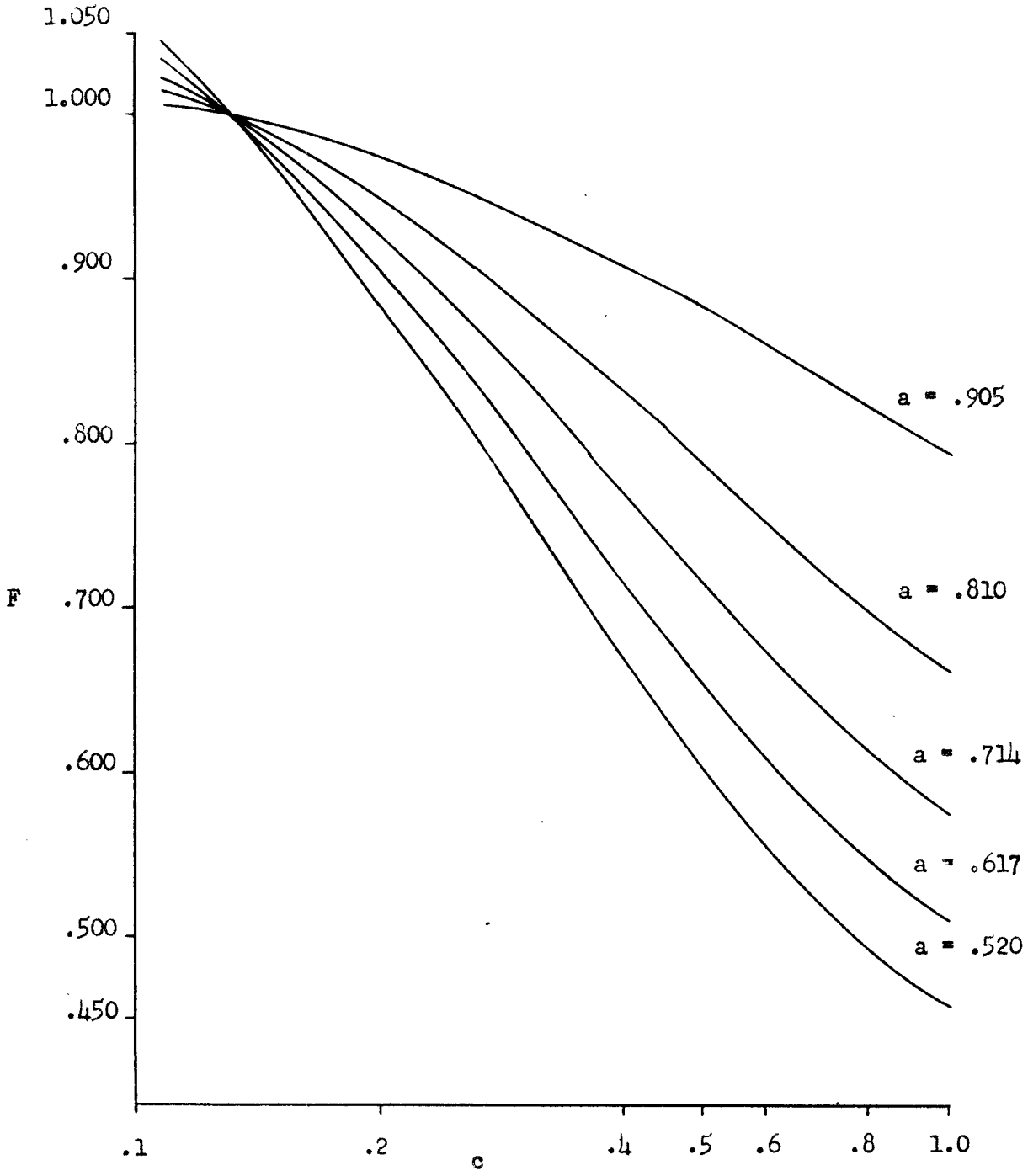

Fig. 4a.--F vs. c with constant a (paraffin medium)

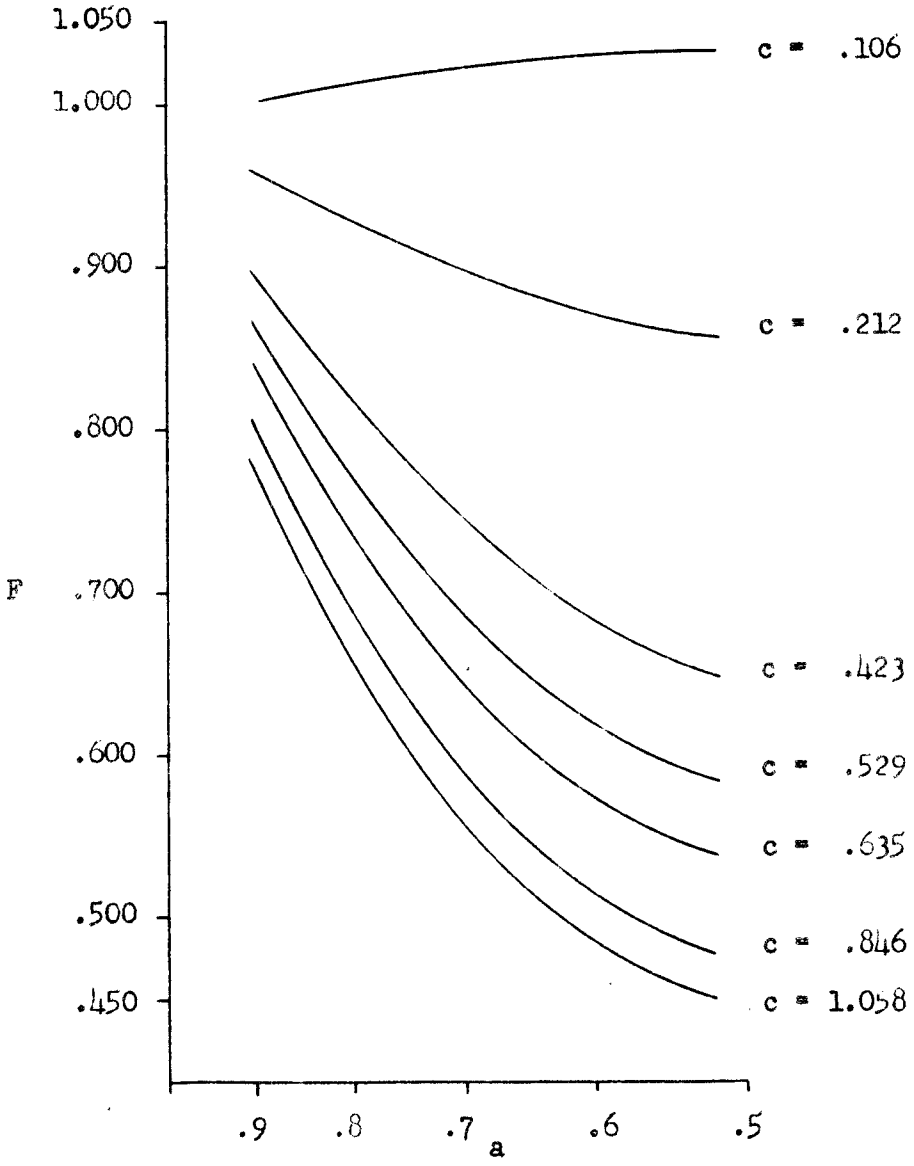

Fig. 4b.--F vs. a with constant c (paraffin medium).

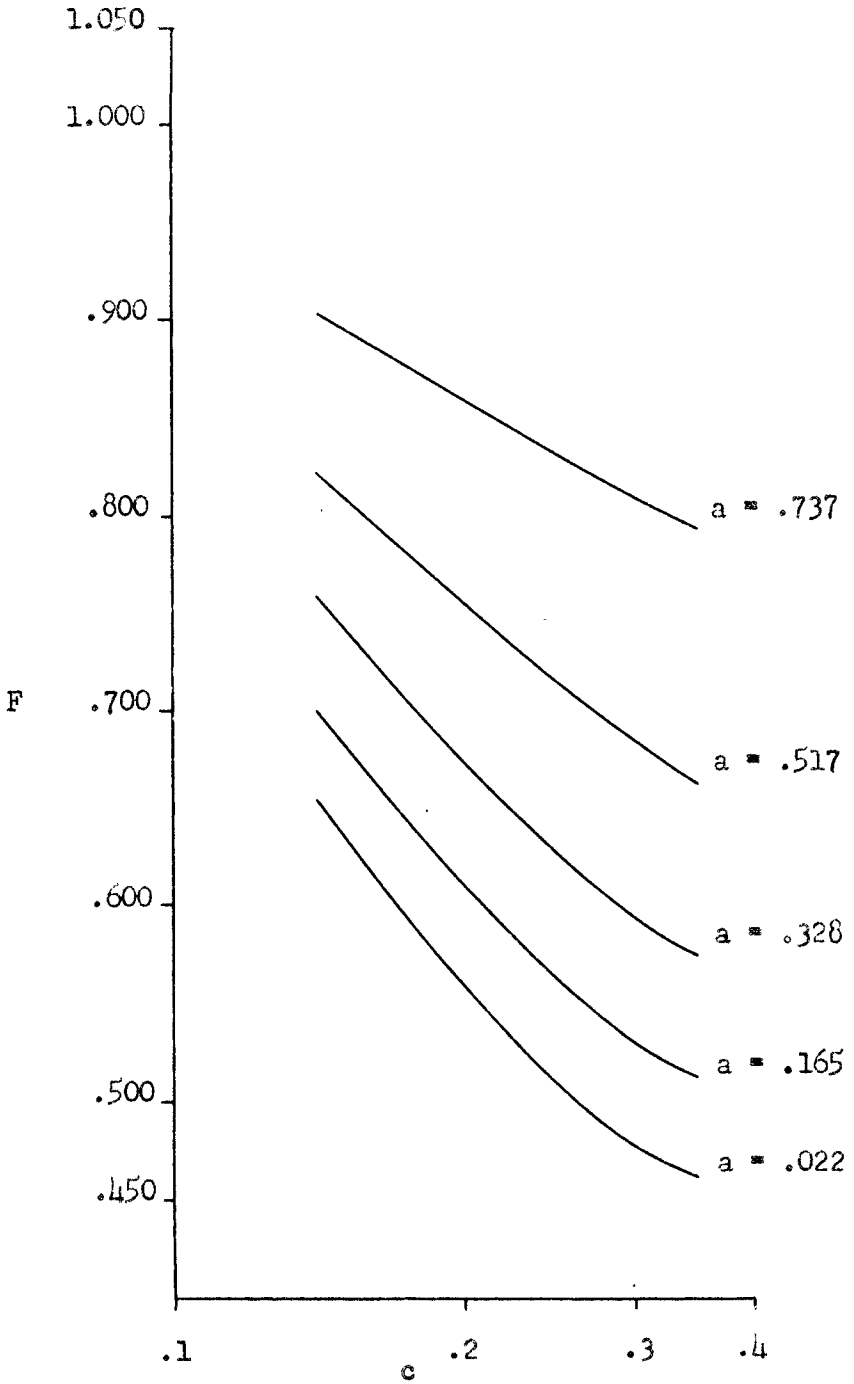

Fig. 5a.—F vs. c with constant a (graphite medium).

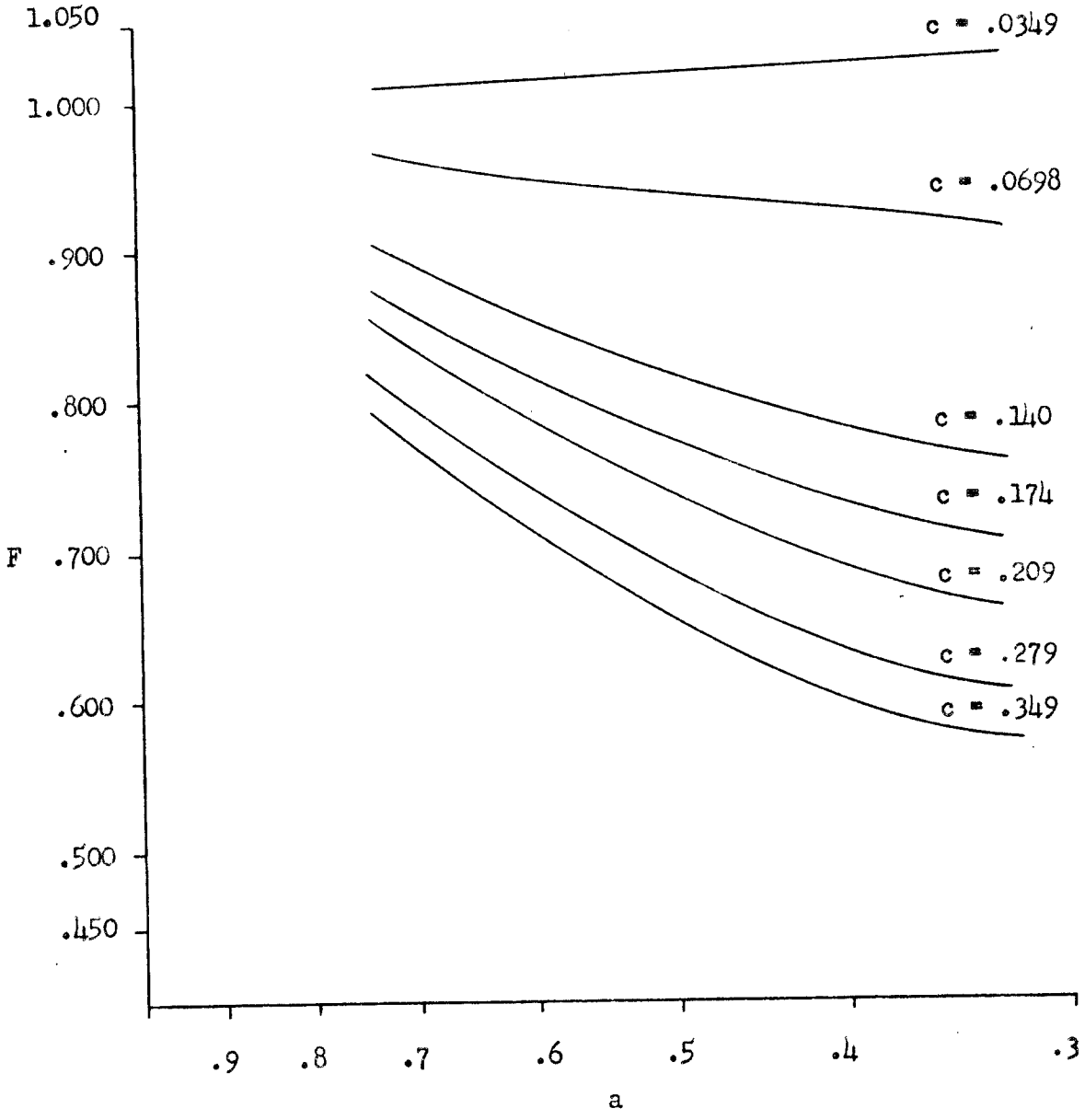

Fig. 5b.—F vs. a with constant c (graphite medium)

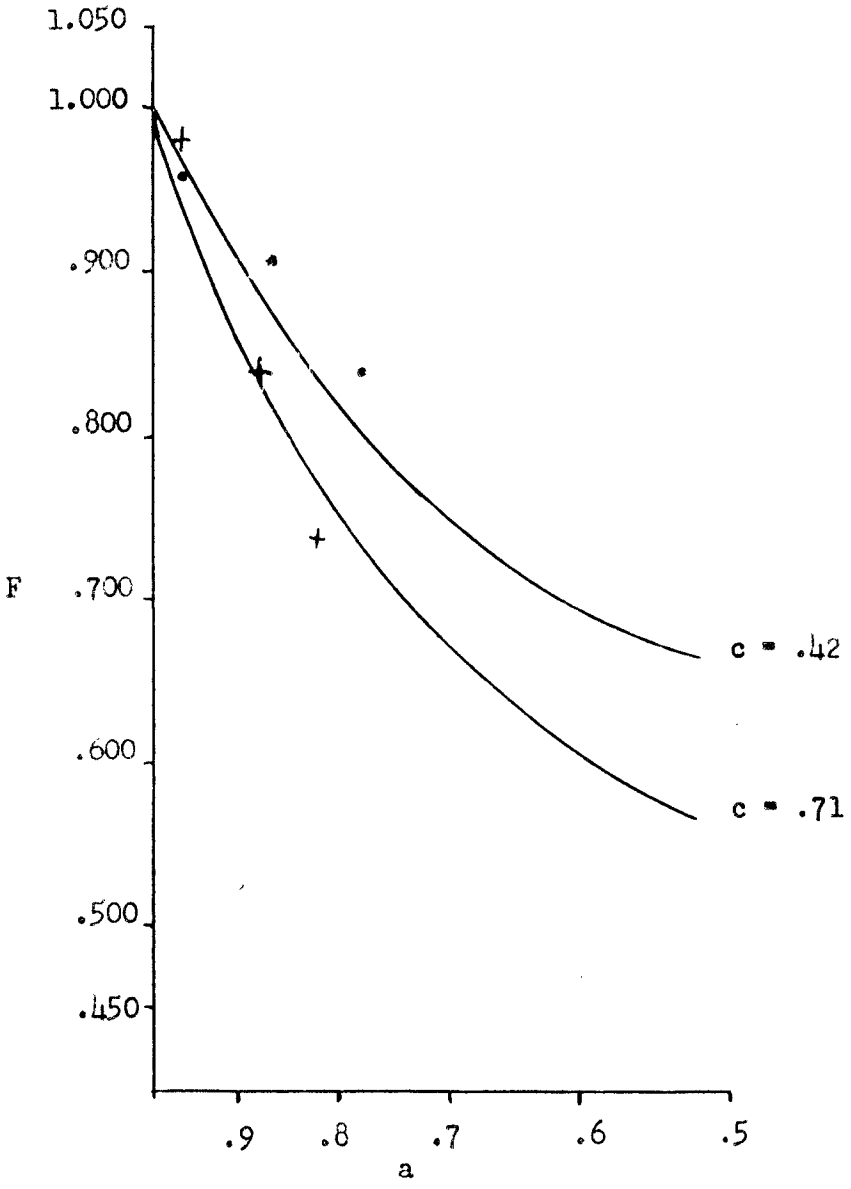

Fig. 6.--F vs. a with constant augmented c. Bothe's experimental data are shown: 0 corresponds to c = 0.42 and + corresponds to c = 0.71.

CHAPTER IV

CONCLUSIONS AND SUGGESTIONS FOR FUTURE STUDY

The results of this paper show that a depression factor can be determined which corresponds to the experimentally determined depression factors by Bothe. However, the experimental data are not extensive and further work on experimental depression factors should be made.

Agreement of theoretical and experimental data indicates, to some degree, the validity of the "simplifying" assumptions which were made in Chapter II. The approximation that a disc could be considered as having a negligible thickness but a finite absorption was quite helpful and does not seem to introduce any large errors in the final results.

A theoretical verification of the augmentation distance of $0.80\lambda_t$ for these geometries would be exceedingly interesting.

BIBLIOGRAPHY

Books

Glasstone, S., and Edlund, M. C., The Elements of Nuclear Reactor Theory, New York, D. Van Nostrand Co., Inc., first edition, 1952.

Morse, P. M., and Feshbach, H., Methods of Theoretical Physics, Part II, New York, McGraw-Hill Book Co., first edition, 1953.

Articles

Bothe, N., Zeit. f. Phys. 120, 437 (1943).

Corinaldesi, E., Nuovo Cim. 3, 131 (1946).

Tittle, C. W., Nucleonics 9, 60 (1951).

Unpublished Material

Trammell, M. R., "Neutron Density Depression Due to an Oblate Spheroidal Detector," Unpublished Master's Thesis, Department of Physics, North Texas State College, January, 1954.

Workman, B. J., "A Method for Calculating Foil Depression Factors," Unpublished Master's Thesis, Department of Physics, North Texas State College, June, 1953.